

# ULTRASHORT OPTICAL PULSE PROPAGATION IN A DOUBLE LAYER OF GRAPHENE BORON NITRIDE WITH ACCOUNTING THE MATERIAL DISPERSION

A. V. Pak<sup>1</sup>, M. B. Belonenko<sup>2</sup>, O. Y. Tuzalina<sup>3</sup>

<sup>1</sup> Volgograd State University, 400062, Volgograd, Russia

<sup>2</sup> Laboratory of Nanotechnologies, Volgograd Institute of Business, 400048, Volgograd, Russia

<sup>3</sup> Volgograd State Agricultural University, 400002, Volgograd, Russia  
pak.anastasia@gmail.com

**PACS 78.20.-e, 78.67 Wj**

The propagation of ultra-short optical pulses in a thin film created by graphene grown on a boron nitride base will be considered, taking into account the environment's dispersion characteristics, electron conduction in such a system described by the framework of an effective long-wave Hamiltonian for low-temperature media. The electromagnetic field is taken as classical Maxwell's. We reveal the dependence of the electric field on the maximum amplitude of ultra-short optical pulses, as well as on empirical dispersion constants.

**Keywords:** graphene, propagation of ultra-short optical pulses, boron nitride base.

## 1. Introduction

Recently, laminated structures based on graphene have attracted the interest of many researchers. Graphene, which grown on the boron nitride base is one of these structures.

Both boron nitride and graphene have hexagonal crystal lattices, that allows the construction of hybrid materials on their basis. This structure is interesting because a boron nitride is an insulator, and graphene is a conductor. It is possible to obtain substances with different band gaps by combining them together in the various ways. Many other authors are interested in both the theoretical and experimental investigations of these structures. [2–11].

The dynamics of ultra-short optical pulses propagating in a double-layer graphene-boron nitride structure were investigated in the hopes that dispersion qualities in non-magnetic environments would be revealed.

## 2. Principal equations

We considered a graphene layer on a boron nitride base. The Hamiltonian we chose in a long-wave approximation, in basis  $\phi_{g1}$ ,  $\phi_{g2}$ ,  $\phi_{nb1}$ ,  $\phi_{nb2}$ , where the wave functions are conformed to an electron, localized on one graphene sub-lattice, on another graphene sub-lattice, on one boron nitride sub-lattice and on another boron nitride sub-lattice accordingly, depicted in matrix view as:

$$H(k) = \begin{pmatrix} 0 & k^* & 0 & t \\ k & 0 & 0 & 0 \\ 0 & 0 & \Delta & f^* \\ t & 0 & f & -\Delta \end{pmatrix} \quad (1)$$

Here,  $t$  — is an electron jumping integral between graphene and boron nitride layers;  $\Delta$  — is a forbidden zone quantity for boron nitride;  $k = v_{fg}(k_x + ik_y)$ ,  $\mathbf{v}_{fg}$  — is the Fermi velocity for graphene;  $k_x, k_y$  — are the electron pulse components;  $\mathbf{f} = \mathbf{v}_{fng}(\mathbf{k}_x + i\mathbf{k}_y)$ ;  $\mathbf{v}_{fng} - \mathbf{v}_{fg}$  — are the Fermi velocity for the boron nitride.

The Hamiltonian (1) we can rewrite, using a block matrix structure [13]:

$$H(k) = \begin{pmatrix} 0 & k^* & 0 & t \\ k & 0 & 0 & 0 \\ 0 & 0 & \Delta & f^* \\ t & 0 & f & -\Delta \end{pmatrix} \equiv \begin{pmatrix} H_{11} & H_{12} \\ H_{21} & H_{22} \end{pmatrix}.$$

For cases when the forbidden zone quantity in the boron nitride is large as compared to the electron's energy, the long-wave approximation can be considered, allowing one to write the effective Hamiltonian by analogy with bigraphene [13]:

$$H^{eff} \equiv H_{11} - H_{12}H_{22}^{-1}H_{21} = -\frac{1}{t} \begin{pmatrix} \Delta & -\frac{1}{t}f^*k^* \\ -\frac{1}{t}fk & -\frac{1}{t^2}|k|^2\Delta \end{pmatrix}. \quad (2)$$

The operated approximation practically is a supplementary limitation on the ultimate electrons pulse, which we can consider within the bounds of a long-wave approximation and match to originally usable a long-wave approximation for electronic graphene sub-system. The Hamiltonian (2) can be easily diagonalized. It gives us the electron spectrum:

$$\varepsilon(k_x, k_y) = \frac{1}{2} \left( \Delta (1 - v_{fg}^2 (k_x^2 + k_y^2)) + \sqrt{\Delta^2 (1 - v_{fg}^2 (k_x^2 + k_y^2))^2 + \frac{4v_{fg}^2 v_{fng}^2}{t^2} (k_x^2 + k_y^2)^2} \right), \quad (3)$$

where  $v_{fg}, v_{fng}$  — are the Fermi velocities of electrons in graphene and boron nitride, respectively.

According to quantum mechanics laws, in the presence of an external electric field  $\mathbf{E}$ , which directed along the  $x$  axis, the gauge can be chosen for the field in the following form:  $\vec{E} = -\partial\vec{A}/c\partial t$ , where  $c$  is the speed of light in a vacuum, we need to change the momentum to a generalized momentum  $p \rightarrow p - eA/c$ , where  $e$  is the electron charge. In this case, the effective Hamiltonian (2) can be written as follows:

$$H = \sum_{p\sigma} \varepsilon \left( p - \frac{e}{c}A(t) \right) a_{p\sigma}^+ a_{p\sigma},$$

where  $a_{p\sigma}^+, a_{p\sigma}$  — are the creation and annihilation operators of the electron with quasimomentum  $p$  and spin  $\sigma$ .

We can write the Maxwell equations without accounting for material dispersion as follows [8]:

$$\frac{\partial^2 \mathbf{E}}{\partial x^2} - \frac{1}{c^2} \frac{\partial^2 \mathbf{E}}{\partial t^2} + \frac{4\pi}{c} \frac{\partial \mathbf{j}}{\partial t} = 0. \quad (4)$$

Here, we neglect the laser-beam diffraction in the directions perpendicular to the beam-propagation axes.

Here,  $\vec{E}$  is an electric field of the light wave,  $t$  is a time,  $C$  is the speed of light in a vacuum.

We modified equation (4) to describe pulse propagation with wide spectrum in a linear medium. The linear refraction index dependence for an isotropic environment  $n$  on

light frequency  $\omega$  in the environment's transparency range can be accurately described by the expression [9]

$$n^2(\omega) = N_0^2 + 2cN_0a\omega^2 + 2cN_0a_1\omega^4 + \dots - 2cN_0b\omega^{-2} - 2cN_0b_1\omega^{-4}, \quad (5)$$

where  $N_0, a, a_1, \dots, b, b_1, \dots$  — are empirical constants of environment dispersion. The dispersion relation (5) gives birth to the wave equation:

$$\frac{\partial^2 \mathbf{E}}{\partial x^2} - \frac{N_0^2}{c^2} \frac{\partial^2 \mathbf{E}}{\partial t^2} = -\frac{2N_0}{c} a \frac{\partial^4 \mathbf{E}}{\partial t^4} + \frac{2N_0}{c} a_1 \frac{\partial^6 \mathbf{E}}{\partial t^6} - \dots + \frac{2N_0}{c} b \mathbf{E} - \frac{2N_0}{c} b_1 \int_{-\infty}^t dt' \int_{-\infty}^{t'} \mathbf{E} dt'' + \dots \quad (6)$$

Equation (5) describes the pulse propagation along the x axis in a forward and a reverse direction.

When comparing equations (4) and (6), taking into account the gauge described above, and limiting oneself by the fourth derivative, one can say that the equation (6); takes the following form:

$$\frac{\partial^2 A}{\partial x^2} + \frac{2N_0}{c} a \frac{\partial^4 A}{\partial t^4} - \frac{2N_0}{c} b A + \frac{4\pi}{c} j - \frac{N_0^2}{c^2} \frac{\partial^2 A}{\partial t^2} = 0. \quad (7)$$

Vector potential  $\mathbf{A}$  has the following form:  $\mathbf{A} = (0, 0, A(x, t))$ .

Written in the standard expression for the current density:

$$j_0 = e \sum_{ps} v_s \left( p - \frac{e}{c} A(t) \right) \langle a_{ps}^+ a_{ps} \rangle, \quad (8)$$

where  $v_s(p) = \frac{\partial \varepsilon_s(p)}{\partial p}$ , and the brackets denote averaging with a non-equilibrium density matrix  $\rho(t)$ :  $\langle B \rangle = Sp(B(0)\rho(t))$ .

Further, we considered the low-temperature case, where only a small area of the pulse space near the Fermi level gives a nonzero contribution to the sum (or integral) of (8).

According to this, we can rewrite the standard expression for the current density as follows:

$$j = e \int_{-\Delta}^{\Delta} \int_{-\Delta}^{\Delta} dp_x dp_y v_y \left( p - \frac{e}{c} A(x, t) \right). \quad (9)$$

The range of pulses integration in (9) can be defined from a view of the equality for the particle:  $\int_{-\Delta}^{\Delta} \int_{-\Delta}^{\Delta} dp_x dp_y = \int_{-\Delta}^{\Delta} \int_{-\Delta}^{\Delta} dp_x dp_y \langle a_{p_x, p_y}^+ a_{p_x, p_y} \rangle$ .

### 3. Numerical simulation results

We solve Eq. (7) numerically using a direct finite-difference cross-like scheme [15]. Stride by time and coordinate are determine by standard conditions of stability, even so, strides of finite-difference scheme are halved serially, until the solution didn't change in  $8^{th}$  sign.

The initial condition is chosen in a view of an ultra-short optical pulse, which was composed of one field oscillation that, accordingly, can be given with using of vector potential  $\mathbf{A}$ :

$$A(x, t) = Q \exp(-(x - vt)^2/\gamma) \\ \gamma = (1 - v^2)^{1/2}, \quad (10)$$

where  $Q$  — is the amplitude, and  $v$  — is the initial ultra-short optical pulse velocity on the sample input.

This initial condition corresponds to the fact, that we deal with the ultra-short optical pulse which is composed of one electric field oscillation.

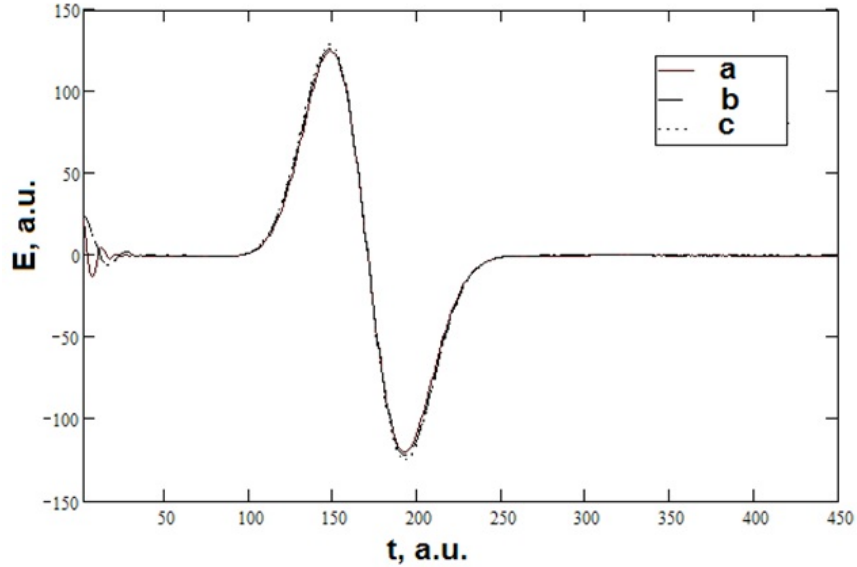


Fig. 1. Dependence of the electric-field on time. On the X-axis is time (unit is  $1 \cdot 10^{-16}$ s), on the Y-axis is electric-field (unit is  $10^8$  V/m).  $a=0.01, b=0.01$ ;  $a=0.1, b=0.3$ ;  $a=0.1, b=0.5$

Values of energy characteristics are shown in  $\Delta$  units. The evolution of the propagating electric field in the sample is presented in Fig. 1.

Such behavior of the optical pulse follows from the dispersion effects, which can be obtained from the linearized equation (7). These effects lead to pulse spreading. It should also be noted that nonlinearity results in pulse shrinking. The impact of these two effects leads to both the origin pulse shape deformation and its propagation in an invariable form.

The most sharply nonlinear influence is tied with the pulse form's dependence on the initial amplitude, that is presented in Fig. 2.

Especially sharp effects are related with the nonlinear influence on the pulse front, leading to pulse widening. This can be explained by the lack of balance between the dispersion and the nonlinearity in our system Fig. 3.

Also notice that the ultra-short optical pulse evolution depend upon, in general, the pulse velocity on the sample input, as shown in Fig. 4.

#### 4. Conclusion

It follows from the obtained results that stable ultra-short optical pulses can undergo propagation in graphene, grown on a hexagonal boron nitride base.

If the initial pulse amplitude increases, then a wave front becomes wider, and also originates a second pulse with smaller intensity. This effect can be useful for the development of hybrid devices based on the light interaction effect with graphene electrons.

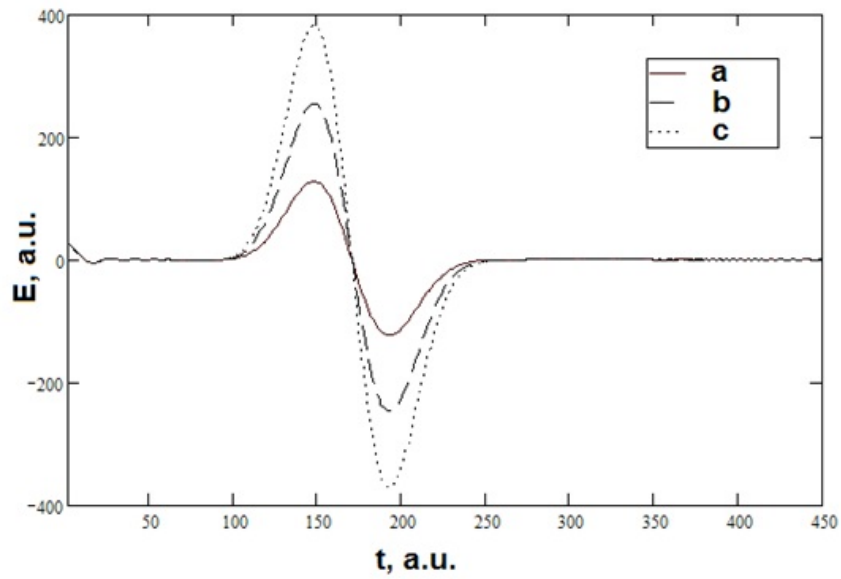


Fig. 2. Dependence of the pulse form on time for different cases of pulse amplitude value: On the X-axis is time (unit is  $1 \cdot 10^{-16}$ s). On the Y-axis is electric-field (unit is  $10^7$  V/m). a)  $Q=2$ ; b)  $Q=4$ ; c)  $Q=6$

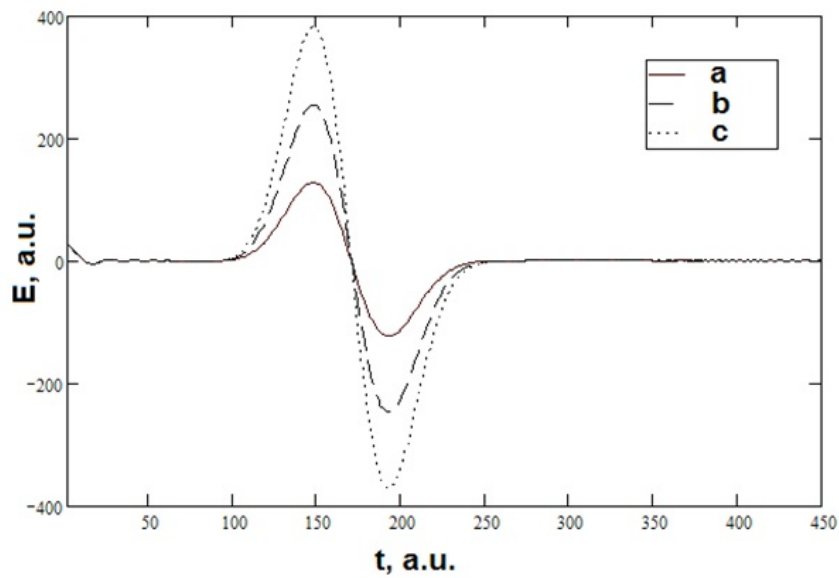


Fig. 3. Dependence of the pulse form on time for different cases of pulse amplitude value: On the X-axis is time (unit is  $1 \cdot 10^{-16}$ s) while the Y-axis is electric-field (unit is  $10^7$  V/m). a)  $Q=2$ ; b)  $Q=4$ ; c)  $Q=6$

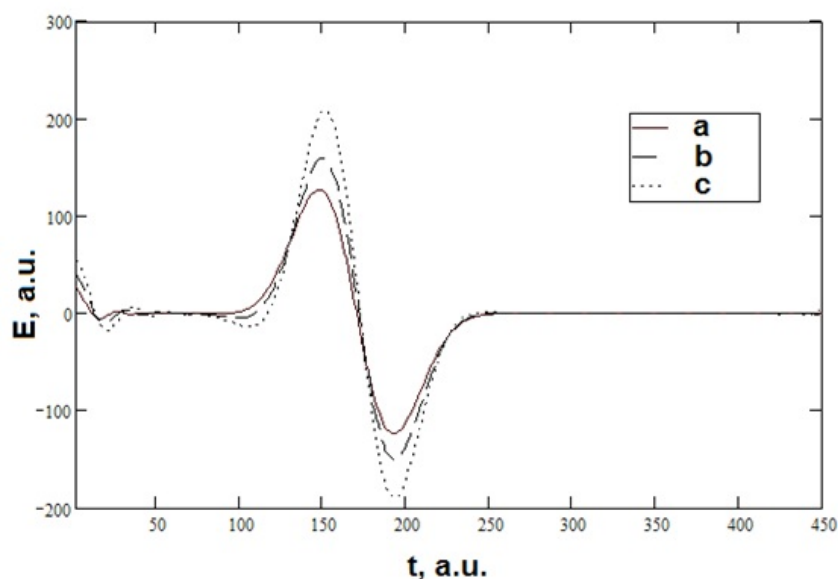


Fig. 4. Dependence of the electric-field on time. On the X-axis is time (unit is  $1 \cdot 10^{-16}$ s), on the Y-axis is electric-field (unit is  $10^8$  V/m). For curve (b) traveled by pulse distance is half as much again as for (a), for curve (c) — twice as much again as for curve (a):  $a=0.1$ ,  $b=0.4$

### Acknowledgements

This work was supported by the Russian Foundation for Basic Research under Project No. 11-02-97054, 12-02-31654.

### References

- [1] Ci L., Song L., Jin C., Jariwala D., Wu D., Li Y.J., Srivastava A., Wang Z.F., Storr K., Balicas L., Liu F., and Ajayan P.M. Atomic layers of hybridized boron nitride and graphene domains. *Nature Materials*, **9**, P. 430–435 (2010). doi:10.1038/nmat2711.
- [2] Giovannetti G., Khomyakov P.A., Brocks G., Kelly P.J., and Van den Brink J., Substrate-induced band gap in graphene on hexagonal boron nitride: *Ab initio* density functional calculations. *Physics Review*, **B 76**, P. 073103 (2007).
- [3] Greber T. *Graphene and boron nitride single layers*. In: Sattler K., editor. The Handbook of Nanophysics. Taylor and Francis Books, Inc, Oxfordshire (2010).
- [4] Partoens B., Peeters F. M. From graphene to graphite: electronic structure around the K point. *Physical Review*, **B 74**, P. 075404-11 (2006).
- [5] Avetisyan A. A., Partoens B., and Peeters F. M. Stacking order dependent electric field tuning of the band gap in graphene multilayers. *Physical Review*, **B 79**, P. 035421 (2009).
- [6] Avetisyan A. A., Partoens B., and Peeters F. M. Electric field control of the band gap and Fermi energy in graphene multilayers by top end back gates. *Phys. Rev.*, **B 80**, P. 195401 (2009).
- [7] Wakabayashi K., Takane Y., Sigrist M. Perfectly conducting channel and universality crossover in disordered graphene nanoribbons. *Physical Review Letters*, **99**, P. 036601 (2007).
- [8] Blase X., Rubio A., Louie S.G., and Cohen M.L. Stability and band-gap constancy of boron-nitride nanotubes. *Europhys Letters*, **28**(6), P. 355–340 (1994).
- [9] Hernández E., Goze C., Bernier P., and Rubio A. Elastic properties of C and  $B_xC_yN_z$  composite nanotubes. *Physical Review Letters*, **80**(20), P. 4502–4505 (1998).
- [10] Chen Y., Zou J., Campbell S.J., and Le Caer G. Boron nitride nanotubes: Pronounced resistance to oxidation. *Applied Physics Letters*, **84**, P. 2430–2432 (2004).
- [11] Suryavanshi A. P., Yu M., Wen J., Tang C., and Bando Y. Elastic modulus and resonance behavior of boron nitride nanotubes. *Applied Physics Letters*, **84**, P. 2527–2529 (2004).

- [12] Breshenan M.S., Hollander M.J., Wetherington M. and al. Integration of hexagonal boron nitride with quasi-freestanding epitaxial graphene: toward wafer-scale, high-performance devices. *ACS Nano*, **6**(6), P. 5234-5241 (2012). DOI: 10.1021/nn300996t.
- [13] Xue J., Sanchez-Yamagishi J., Bulmash D., Jacquod Ph., Deshpande A., Watanabe K., Taniguchi T., Jarillo-Herrero P., LeRoy B.J. Scanning tunneling microscopy and spectroscopy of ultra-flat graphene on hexagonal boron nitride. *Nature Materials*, **10**, P. 282–285 (2011).
- [14] Cortijo A., Guinea F., Vozmediano M.A.H., Geometrical and topological aspects of graphene and related materials. arXiv: 1112.2054v1 (2011).
- [15] Landau L. D., Lifshitz E. M. *Theoretical physics*, T. II. Field theory, Science, Moscow, 512 p. (1988).
- [16] Bakhvalov N.S. *Calculus of approximations (analysis, algebra, ordinary differential equations)*. Science, Moscow, 632 p. (1975).